

Logic-Based Active Control of Subsonic Cavity Flow Resonance

M. Debiasi* and M. Samimy†
The Ohio State University, Columbus, Ohio 43210

We present the results of an experimental investigation for controlling a shallow cavity flow in the Mach number range 0.25–0.5. The flow exhibits the characteristic staging behavior predicted by the semi-empirical Rossiter formula with multiple modes in the Mach number range 0.32–0.38 and a single strong mode in other Mach numbers. A survey of the velocity at the exit of the zero net mass flow compression-driver actuator used for control reveals that its amplitude is frequency dependent and its behavior is little influenced by the main flow. Forcing the Mach 0.3 flow indicated that the actuator has good authority over a large range of frequencies, with reduction of spectral peaks observed at some forcing frequencies. We took advantage of this phenomenon to develop a logic-based controller that searches the frequency space and maintains the optimal forcing frequency for peak reduction at each Mach number. Optimal frequencies and the corresponding reduced resonance have been obtained for all of the flow conditions explored. The physics of optimal frequency forcing as well as some characteristics of the logic-based controller are discussed.

I. Introduction

APPPLICATION of closed-loop control in fluid dynamics is by its nature a challenging and fascinating problem. Although many significant results have been obtained with open-loop flow control, this technique lacks the responsiveness or the flexibility needed for application in dynamic flight environments. In contrast, closed-loop flow control, although in its infancy, appears to be the ideal technique for the successful management of flow in many applications due to its adaptability to variable conditions and to its potential for significantly reducing the power required for controlling the flow. For example, Cattafesta et al.¹ found that closed-loop control of cavity tones requires an order-of-magnitude less power than open-loop control.

The results presented here are part of a larger multidisciplinary effort to develop tools and methodologies that can apply closed-loop aerodynamic flow control for manipulating the flow over maneuvering air vehicles. The first step was to select a particular flowfield relevant to Air Force applications and to utilize it in the development of various components of closed-loop flow control techniques. The case study chosen is the control of shallow cavity flow pressure fluctuations that are characterized by a strong resonance produced by a natural feedback mechanism similar to that occurring in other flows with self-sustained oscillations (e.g., impinging jet, screeching jet). In all of these cases, shear layer structures impacting a discontinuity or obstacle in the flow (e.g., the cavity trailing edge) scatter acoustic waves that propagate upstream and reach the shear layer receptivity region where they tune and enhance the development and growth of shear layer structures. In the case of flow over a weapon bay cavity, these fluctuations can lead to structural damage to the air vehicle or to the stores carried within the bay.

Rossiter² first developed an empirical formula for predicting the cavity flow resonance frequencies, today referred to as Rossiter frequencies or modes. He also investigated the concept of a dominant mode of oscillation. Later Rockwell and Naudascher³ observed that this dominant mode tends to coincide with that of

the natural longitudinal cavity resonance. Williams et al.⁴ confirmed that Mach numbers at which single-mode resonance occurs are located at the intersections of the first longitudinal cavity mode with one of the Rossiter modes, whereas Mach numbers for multimode resonance fall between the single-mode resonance conditions. Rapid switching between modes has been observed in multimode conditions.^{4–6} Joint time-frequency analysis (short-time Fourier transform, wavelet analysis, and bispectral analysis) capture this phenomenon.⁵ The random switching between multiple modes on a rapid timescale places large bandwidth and fast time response requirements on the actuation scheme and feedback control algorithm.^{4,5}

Extensive work has been done on controlling the flow over a cavity. In general, control techniques that do not add energy to the flow are considered passive; otherwise they are active.⁷ Passive techniques rely on geometrical modification by using rigid fixed fences, spoilers, ramps,^{8–10} passive bleeding systems,¹¹ steady mass injection,¹² and cylinders or rods placed in the boundary layer near the leading edge of the cavity.^{10,13,14} Passive devices are simple, inexpensive, and reliable, but often they may not work well at off-design conditions because they have limited or no capability to adjust themselves to changing flow requirements. Active control techniques, on the other hand, are more complex and expensive but can self-adjust to the flow needs. They can be further divided into closed and open-loop schemes depending on whether feedback information from the system is used to modify the control signal.^{7,15} Different open-loop^{9,16,17} and closed-loop^{1,4,6,18–24} approaches have been used in the control of cavity flow. The results of these endeavors are encouraging but also indicate that many issues remain to be solved. For example, suppression of resonant tones is often accompanied by either peak splitting, i.e., creation of a pair of lower-magnitude tones on either side of the suppressed one,^{21,22} or peaking, where acoustic energy reappear away from the original tone(s).^{21,25} Therefore many opportunities remain for further advancement of the technology.²⁶

Actuation is a crucial element of any active control work. Flow forcing is divided into two categories, low-frequency forcing and high-frequency forcing; the latter is characterized by forcing at frequencies an order of magnitude larger than the frequency associated with the phenomenon to be controlled.¹² For cavity flow control, the requirement for low-frequency forcing devices is a bandwidth that includes the Rossiter frequencies of interest.²⁷ Candidate low-frequency actuators include piezoelectric flaps with deflections on the order of the viscous sublayer of the boundary layer approaching the cavity,^{1,20} steady and pulsating blowing jets,^{9,16–18,28} and synthetic jets that add momentum to the flow without mass addition.^{4,6,21–24} Stanek et al.²⁹ successfully demonstrated cavity tone suppression across a broad range of frequencies without

Presented as Paper 2003-4003 at the AIAA 33rd Fluid Dynamics Conference, Orlando, FL, 23–26 June 2003; received 26 August 2003; revision received 6 February 2004; accepted for publication 29 February 2004. Copyright © 2004 by the American Institute of Aeronautics and Astronautics, Inc. All rights reserved. Copies of this paper may be made for personal or internal use, on condition that the copier pay the \$10.00 per-copy fee to the Copyright Clearance Center, Inc., 222 Rosewood Drive, Danvers, MA 01923; include the code 0001-1452/04 \$10.00 in correspondence with the CCC.

*Postdoctoral Researcher, Gas Dynamics and Turbulence Laboratory, Collaborative Center of Control Science. Member AIAA.

†Professor, Gas Dynamics and Turbulence Laboratory, Collaborative Center of Control Science; Samimy.1@osu.edu. Associate Fellow AIAA.

exciting additional tones at supersonic speeds by using a powered resonance tube, a high-frequency fluidic device whose frequency is an order of magnitude greater than the Rossiter modes (see Refs. 30–32). These fluidic actuators are not well suited to closed-loop flow control at the present time, as they cannot be phase locked.

In this work we present the experimental results in cavity flow control obtained to date at the Gas Dynamics and Turbulence Laboratory (GDTL) of the Ohio State University. For this purpose a small subsonic wind tunnel with a shallow cavity has been built and tested and the flow resonance in the Mach number range 0.25–0.5 has been explored. The tunnel with the current arrangement can operate continuously up to about Mach 1. A synthetic-jet type of actuation is used to force the shear layer at its receptivity region. A titanium-diaphragm compression driver, capable of large bandwidth and great flexibility in the generation of sound, drives the actuator. A preliminary study of the actuator characteristics without and with main Mach 0.3 flow is presented, and the effect of sinusoidal actuation frequency on the Mach 0.3 flow is investigated. Based on the results obtained, a logic-based type of controller has been developed that searches in a closed-loop fashion the frequencies that reduce the cavity flow resonant peaks and then maintains the system in such conditions. The technique performed well in the experimental trials and allowed identification of optimal frequencies for the reduction of resonant peaks in the Mach number range explored.

In the next sections we introduce the flow facility used in this study and then focus on the measurements of the baseline flows, the behavior of the actuator, the effect of forcing frequency, and the design and use of the logic-based controller for reducing the resonance. In each section we describe the experimental procedure and present the results obtained. In the final section we discuss in more detail some of the findings, with particular emphasis on the characteristics of optimal frequency forcing.

II. Flow Facility

A modular, optically accessible experimental facility has been designed and fabricated at the GDTL of the Ohio State University. The facility is of the blow-down type and operates with air supplied by two four-stage compressors allowing continuous operation in the subsonic range. The air is filtered, dried, and stored at 16 MPa in two high-capacity tanks. The air is conditioned in a stagnation chamber before entering the test section through a smoothly contoured converging nozzle. The total pressure in the stagnation chamber can be controlled within 70 Pa (0.07% of the test section static pressure). The test section is square with width $W = 50.8$ mm (2 in.). The upper wall of the test section is adjustable to compensate for the growth of the boundary layer and of the shear layer. A variable-depth cavity that spans the entire width of the test section is recessed in the floor. In the current experiments, the cavity depth D is 12.7 mm (0.5 in.) and its length L is 50.8 mm (2 in.) for an aspect ratio $L/D = 4$. A schematic of the test section with the cavity and the actuator is shown in Fig. 1.

The actuator is a two-dimensional synthetic-jet type issuing from a high-aspect-ratio converging nozzle embedded in the cavity leading edge as shown in Fig. 1. This contoured, 108-mm-long nozzle has a volume of approximately 160 cm³ and exhausts at an angle of 30 deg with respect to the main flow through a slot of width $W = 50.8$ mm (the cavity span) and height $h = 1$ mm. Actuation is provided by the movement of the titanium diaphragm of a Selenium D3300Ti compression driver whose voltage signal is amplified by a Crown D-150A amplifier. This device is conceptually similar to the unsteady bleed actuator used by Williams et al.^{4,6} and Ziada et al.²⁴ for a similar purpose and by McCormick³³ for boundary layer-separation control. The compression-driver diaphragm is capable of oscillating in the frequency range 1–20 kHz. When used as it was designed for, connecting it to an acoustic diffuser for sound production, the device has in this range a relatively flat frequency response. When used in connection to a straight tube, the frequencies in the 500–3000-Hz range are exalted. In the rather unconventional arrangement of our experiments, where the compression driver is connected to a highly converging nozzle, we expect a highly frequency-dependent behavior where some frequencies are

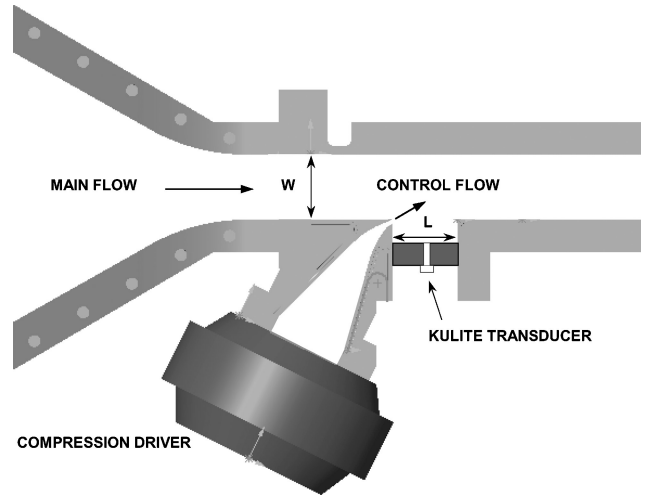


Fig. 1 Cutout of the facility showing the converging nozzle, the test section, the cavity, the actuator coupling, and the placement of the Kulite transducer.

reinforced while others are reduced. This has been verified by the preliminary measurements of the velocity at the exit slot.

III. Cavity Flow Measurements

Preliminary static and dynamic pressure measurements in the Mach number range 0.25–0.5 have been carried out. Measurements of the static pressure at various locations were used to adjust the upper wall, to change the height of the test section, and so to maintain a uniform pressure close to the ambient value along the test section. A slight drop of the static pressure (less than 1% at Mach 0.5, smaller at lower Mach number) is always detected over the cavity and is caused by the growing shear layer that locally reduces the cross section of the tunnel and accelerates the flow. At Mach 0.5 a discrepancy less than 1.3% exists between the test-section nominal Mach number and the average Mach number obtained from measurements over the cavity.

Flow velocity profiles have been measured using a miniature pitot probe (0.8-mm tip diameter) traversing the test section in the horizontal and vertical planes 6.35 mm (0.25 in.) upstream of the cavity leading edge. For all of the flow conditions the boundary-layer thickness at this location is about 2.5 mm both in the vertical and in the horizontal planes and follows a $1/n$ power-law profile with $n = 6$. The flow outside the boundary layer is very uniform across the test section. The Reynolds number based on the cavity step height is 10^5 and based on the boundary layer thickness is 2×10^4 . Further details on the quality of the flow can be found in Samimy et al.³⁴

A complete survey of the cavity flow resonance in the Mach number range 0.25–0.5 was performed using a Kulite XTL-190-25A dynamic pressure transducer with frequency response up to 50 kHz flush-mounted in the middle of the cavity floor (Fig. 1). Recordings consisting of 409,600 samples each were acquired at a sampling frequency of 200 kHz through a 16-bit resolution acquisition board (National Instruments PCI-6036E). Each recording was band-pass filtered between 200 and 20,000 Hz to remove spurious frequency components. By using the Kulite sensitivity of 5.8×10^{-4} mV/Pa (4 mV/psi) and accounting for the amplifier gain setting, the recorded voltages were converted to nondimensional pressure referenced to the commonly used value of $20 \mu\text{Pa}$. Fifty narrowband power spectra, each from 8192 points, were computed using fast Fourier transform with Hanning window, converted to sound pressure level (SPL) spectra, and then averaged. The resulting spectra have a spectral resolution of about 24 Hz and are accurate within ± 1 dB.

The spectral peaks were compared with the cavity flow resonant frequencies predicted using the semi-empirical formula of Rossiter²:

$$Sr_n = \frac{f_n L}{U_\infty} = \frac{n - \varepsilon}{M_\infty \left\{ 1 + [(\gamma - 1)/2] M_\infty^2 \right\}^{-1/2} + 1/\beta} \quad (1)$$

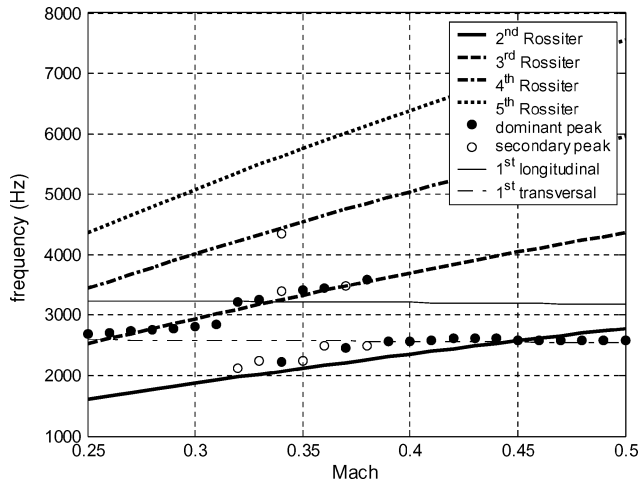


Fig. 2 Rossiter frequencies (thick line), cavity first longitudinal and transversal frequencies (thin line), and measured frequencies (circles) as a function of the flow Mach number.

where n is an integer mode number corresponding to the number of vortices spanning the cavity length L ; U_∞ and M_∞ are the freestream velocity and Mach number; ε is the phase lag (in fraction of a wavelength) between the interaction of a large scale structure in the shear layer with the cavity trailing edge and the formation of a corresponding upstream traveling disturbance (phase shift of the acoustic scattering process); and $\beta = U_c/U_\infty$ is the ratio of the convective speed of the large-scale structures to the freestream velocity. The predicted Rossiter frequencies of our setup ($L = 50.8$ mm) with $\varepsilon = 0.25$ and $\beta = 0.66$ are presented in Fig. 2 as a function of the flow Mach number. Circles in the figure represent the frequency of the resonant peaks measured in our experimental setup. More specifically, closed circles represent dominant peaks, and open circles represent other peaks appearing in multimode resonance. Shown also are the frequencies of the cavity first longitudinal mode and transversal (vertical) mode.

Our experimental setup exhibits strong, single-mode resonance in the Mach number ranges 0.25–0.31 and 0.39–0.5 and multimode resonance in the Mach number range 0.32–0.38. The pressure spectra at selected Mach numbers shown in Fig. 3 illustrate this point more clearly. At Mach numbers 0.26 and 0.29 (Figs. 3a and 3b), a single peak dominates the spectrum by as much as 20 dB over the other spectral components. A similar effect is observed at Mach numbers 0.43 and 0.46 (Figs. 3e and 3f), where a single resonant peak with a distinct first harmonic dominates the other components by as much as 30 dB, as expected for these more energetic, higher-Mach-number flows. Conversely at Mach numbers 0.32 and 0.37 (Figs. 3c and 3d), we observe the presence of multiple smaller peaks that do not exceed significantly the other spectral components. Consistent with previous experimental observations,^{4–6} in multimode resonance the energy available for generation of the acoustic tones had been split among the rapidly alternating peaks instead of concentrating on a single large peak.

Figure 4 complements the preceding figures by showing the intensity of the highest spectral peak as function of the flow Mach number. The dotted line represents the average intensity of the spectral components between 0.2 and 1 kHz. This low-frequency noise plateau, whose intensity increases almost linearly with Mach number, comprises the strongest spectral components that would be observed if the flow was nonresonating.

IV. Velocity Measurements at the Actuator Exit Slot

To assess the behavior of the actuator without and with an external flow, velocity measurements at the exit slot were performed using a TSI 1276-10A subminiature hot-film probe connected to a TSI 1750 constant-temperature anemometer. The 25- μm -thick and 0.25-mm-long sensor has a flat frequency response up to about 40 kHz. The voltage time trace from the anemometer was sampled at 200 kHz

and converted into velocity according to our wind-tunnel calibrations that match within ± 0.25 m/s the one (that has uncertainty less than $\pm 4\%$) provided by the manufacturer for the same probe–anemometer setup and velocity range. Measurements were made without and with a main Mach 0.3 flow by placing the probe in the middle of the exit slot, i.e., at equal distance between the upper and the lower nozzle lips, which are separated by 1 mm. To verify the spanwise uniformity of the jet, measurements were done at the test-section centerline (i.e., 25.4 mm away from both of the side walls) as well as closer to the side wall but outside the boundary layer (6.35 mm from the wall). No difference was detected between the center and off-center measurements both without and with the main flow. Figures 5 and 6 summarize the most relevant findings from the hot-film velocity measurements.

Figure 5 compares excerpts of the derectified velocity time traces at the actuator exit slot for sinusoidal excitation at 1.6 kHz, 5 V_{rms} without and with the Mach 0.3 main flow. The derectified velocity signals presented here closely parallel those obtained by Seifert and Pack³⁵ at the forcing slot of a comparable zero-mass-flux, oscillatory blowing actuator. Analogous time traces were observed at the other actuation frequencies with velocity values varying with frequency and decreasing at lower excitation voltages. Note that the addition of the Mach 0.3 main flow does not alter significantly the velocity time trace at the exit slot except for adding some small, irregular velocity oscillations. Similar behavior has been observed with actuation at lower voltages. However, the effect of the main flow becomes prominent with lower excitation voltages.

Figure 6 shows the variation of the positive-velocity peak at the actuator exit slot with the frequency of sinusoidal excitation for various rms voltages in the absence of main flow. As expected, the actuator behavior is highly frequency dependent with several peaks and valleys in the explored range of 1–10 kHz. This confirms the preliminary observations of resonant dynamics within the actuator nozzle reported by Samimy et al.³⁴ based on measurements of the actuator flow rms velocity obtained with the miniature pitot probe. Conversely, at all frequencies the amplitude response is approximately a linear function of the input voltage level. The positive-velocity peaks in excess of 20 m/s observable at some frequencies and forcing voltages in Fig. 6 compare well with those observed by Seifert and Pack,³⁵ Chen et al.,³⁶ and Guy et al.³⁷ using high-aspect-ratio rectangular synthetic jets. Addition of the Mach 0.3 main flow changes this behavior little for excitation at 4–5 V_{rms} but impacts the behavior at lower voltage settings where the instantaneous values of the velocity are heavily distorted by the main flow.

V. Effect of Actuation Frequency on Mach 0.3 Resonant Flow

Having verified that, at least for operation at higher voltages, the behavior of the actuator is lightly affected by the presence of the main Mach 0.3 flow, we explored the effect of the actuation frequency on this flow. In an attempt to isolate the influence of frequency from that of amplitude, the actuator voltage was manually adjusted with the varying frequency so to maintain, as much as possible, a positive velocity peak of about 5 m/s at the forcing slot.

Figure 7 illustrates some relevant forced cases at different frequencies in comparison with the baseline case. In all cases the thin line, representing the original Mach 0.3 cavity flow spectrum, is displaced 20 dB above the line of the forced one to avoid the overlapping of important spectral features. The baseline flow is characterized by a single resonant peak of 132 dB at 2.8 kHz. With forcing at 2.0 kHz (Fig. 7a), the resonant peak is suppressed while a strong peak appears at the actuation frequency, an indication that the natural feedback has been interrupted and the system has been tuned to the actuator frequency. As expected, actuation at the resonant frequency (Fig. 7b) has the effect of reinforcing the natural feedback and increases the resonant peak by about 8 dB. However, forcing at 3.0 kHz, a frequency just slightly above resonance (Fig. 7c), produces the same effect noticed in Fig. 7a, the system

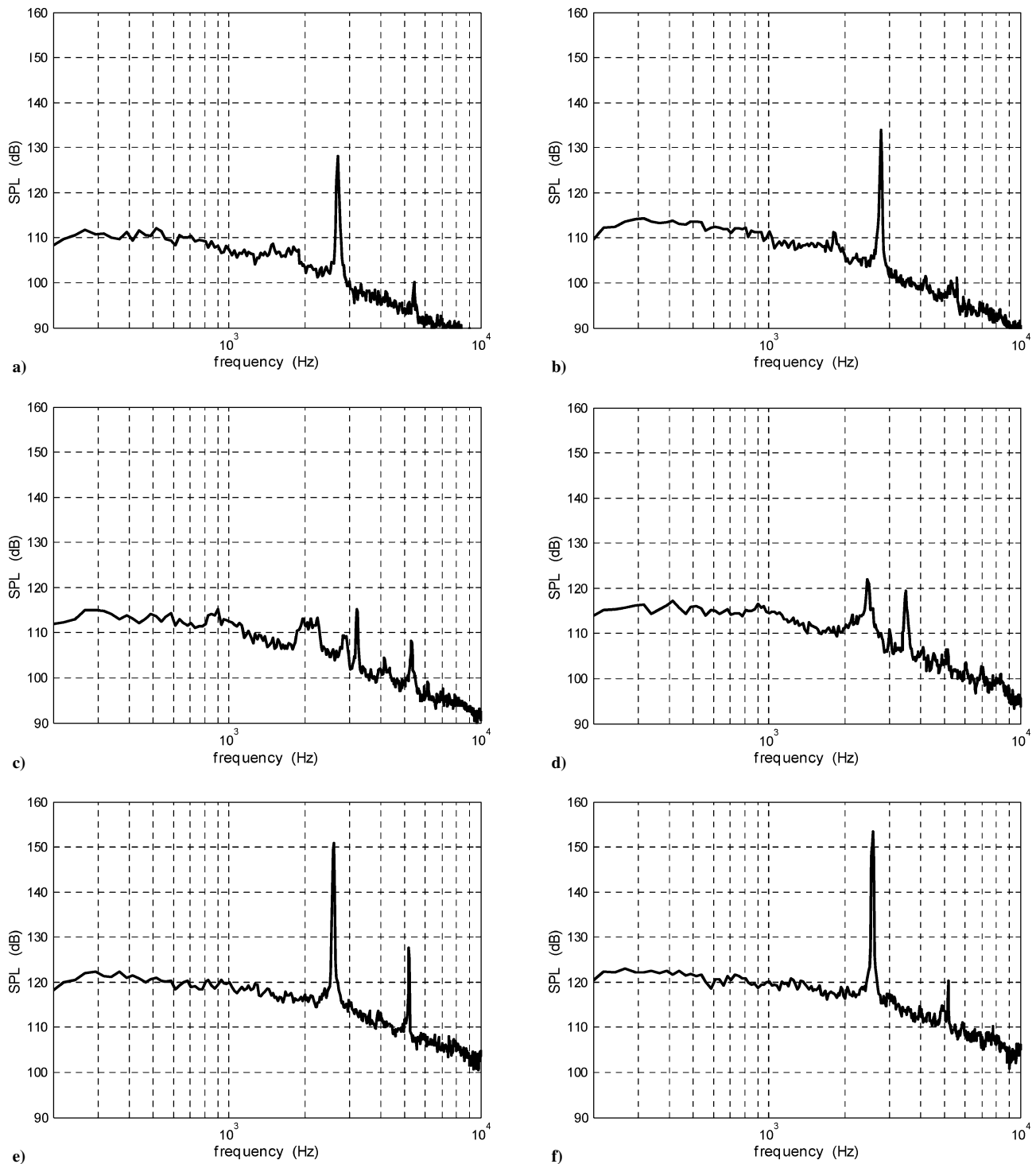


Fig. 3 Cavity flow pressure spectra at selected Mach numbers $M =$ a) 0.26, b) 0.29, c) 0.32, d) 0.37, e) 0.43, and f) 0.46.

being tuned to the forcing frequency with disruption of the original resonant feedback loop. The same effect has been observed with forcing at the majority of frequencies between 2000 and 5000 Hz. In fact the actuator exhibited good authority and produced conspicuous results even at the frequencies corresponding to the “valleys” of Fig. 6 where the maximum forcing velocity is less than 5 m/s. For instance, Fig. 7d presents an interesting case where actuation at 3.25 kHz with peak velocity of about 3 m/s reduced the resonant peak by 18 dB without introducing a strong peak of its own. This occurrence, observed also for actuation at about 3.9 kHz (not presented here), is further discussed in Sec. VII. This remarkable finding has

been used to design a preliminary type of controller for reducing the resonant peaks as described in the next section. Conversely, forcing at frequencies above 5.0 kHz, e.g., 6.25 kHz in Fig. 7e, has a smaller effect on the resonant peak that is reduced but remains comparable to the forcing one. Even higher frequencies show no effect on the resonant peak that remains practically unchanged alongside the forcing tone, as shown for actuation at 9.8 kHz in Fig. 7f. We finally observe that, whereas the forcing frequency may significantly affect the resonant peak, it seems to have little or no effect on the other spectral components, particularly the low-frequency noise plateau.

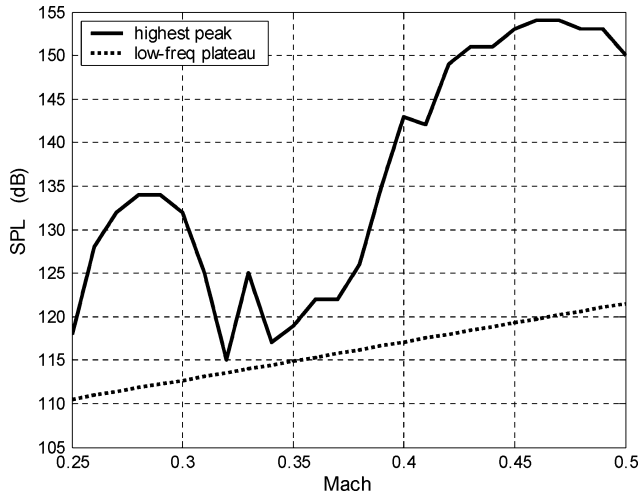


Fig. 4 Intensity of the cavity flow highest spectral peak and of the low-frequency noise plateau as a function of the flow Mach number.

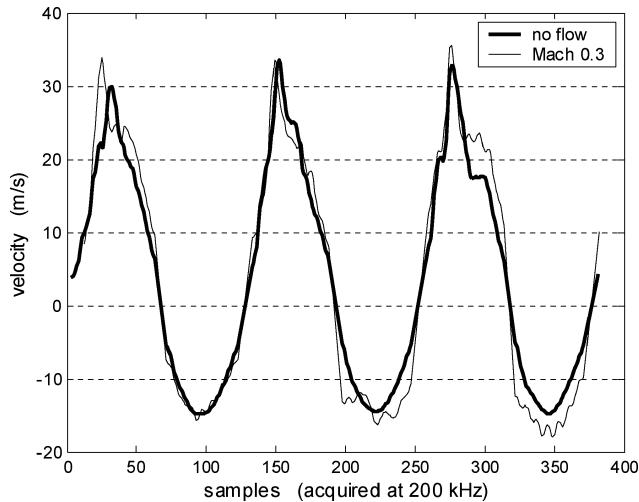


Fig. 5 Derectified time traces of the velocity at the actuator exit slot for sinusoidal excitation at 1.6 kHz, 5 V_{rms} without and with Mach 0.3 main flow.

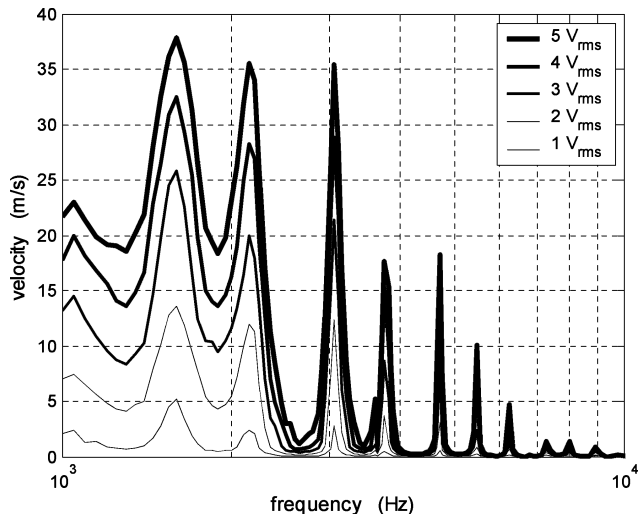


Fig. 6 Variation of the positive velocity peak at the actuator exit slot with the frequency of sinusoidal excitation for various rms voltages in the absence of main flow.

VI. Logic-Based Active Controller for Reduction of Cavity Flow Resonance

Based on what was discovered in regard to the results in Fig. 7d, we decided to develop an automated routine that finds the forcing conditions, if any, for which at a given Mach number from 0.25 to 0.5 the spectral peaks are eliminated or significantly reduced. To simplify the process, we explored the effect of one forcing parameter at a time starting from the frequency that, from what discussed earlier, appears to have the most significant effects. This quite naturally evolved into the logic-based process illustrated in Fig. 8 that can be considered a simple controller for reducing cavity flow resonance, which provided us with valuable information on controllability of the flow and authority of the actuator.

This controller explores the forcing frequency f_f within a specified range, for instance, between 2 and 5 kHz, with increments Δf of 50 Hz. At each value of f_f , the actuator input is a sinusoidal voltage signal of fixed amplitude:

$$V_f = A \sin(2\pi f_f t) \quad (2)$$

After a short time (50 ms) has passed to ensure achieving a statistically steady flow, the pressure fluctuations are measured by the Kulite pressure transducer in the cavity floor and a SPL spectrum is computed as explained in Sec. III. The controller then searches the maximum spectral value SPL_{\max} and compares it with a preset, desired value SPL_{set} . If $SPL_{\max} < SPL_{\text{set}}$, the controller has found a forcing frequency f_f for which the preset requirement is satisfied and therefore stops exploring other forcing frequencies and maintains the excitation at the current value of f_f . Otherwise, the controller continues the exploration of forcing frequencies in the specified range. If no forcing frequency has been found for which the spectral components fall below SPL_{set} , the controller settles for the forcing frequency $f_{f,\text{min-peak}}$ for which the lowest spectral peak has been observed and maintains excitation at that frequency.

In essence the controller operates in a closed-loop fashion by using feedback information (pressure fluctuations) from the flow until it has found a satisfying forcing frequency, after which it converts to an open-loop scheme. In fact, this process is embedded into an additional outer loop that continuously monitors the state of the overall system and triggers a new search if some significant changes are detected, such as an increase in the spectral intensity or a variation of the flow Mach number. This control technique performed remarkably well in our experiments as it was able to find and maintain forcing frequencies reducing strong cavity flow resonant peaks in the entire range of Mach number explored. Furthermore, it proved to be a powerful tool for extracting valuable information in a large range of forcing conditions as discussed next.

First, it should be noted that, as was already mentioned in the discussion of Fig. 7d, sometimes more than one forcing frequency f_f exists for which a significant peak reduction is achieved. From here on we restrict our discussion to the forcing frequencies, which we call “optimal,” that cause the largest peak reduction for each flow Mach number and excitation voltage. In most cases, these frequencies were unequivocally identified by the control routine irrespective of the initial forcing frequency and direction selected for the frequency-sweep process.

Figure 9 shows the optimal frequencies as a function of the flow Mach number with actuator excitation voltages of 5, 4, 3, and 2 V_{rms}. Similar to Fig. 2, the circles represent the measured resonant frequencies and the thin lines the Rossiter frequencies and the frequency of the cavity first longitudinal and transversal modes. The optimal frequency varies somewhat with the excitation voltage at each Mach number, but a general trend is still recognizable, which is characterized by jumps at some Mach numbers. This is not completely surprising because, like other self-sustained resonant flows, the cavity resonance is distinguished by a staging behavior as evidenced by the nature of the Rossiter modes. Based on the results presented in Fig. 9, a simpler controller, embedded into an outer loop continuously monitoring the system, could be devised that directly selects the optimal frequency and voltage for control of the flow for each given Mach number.

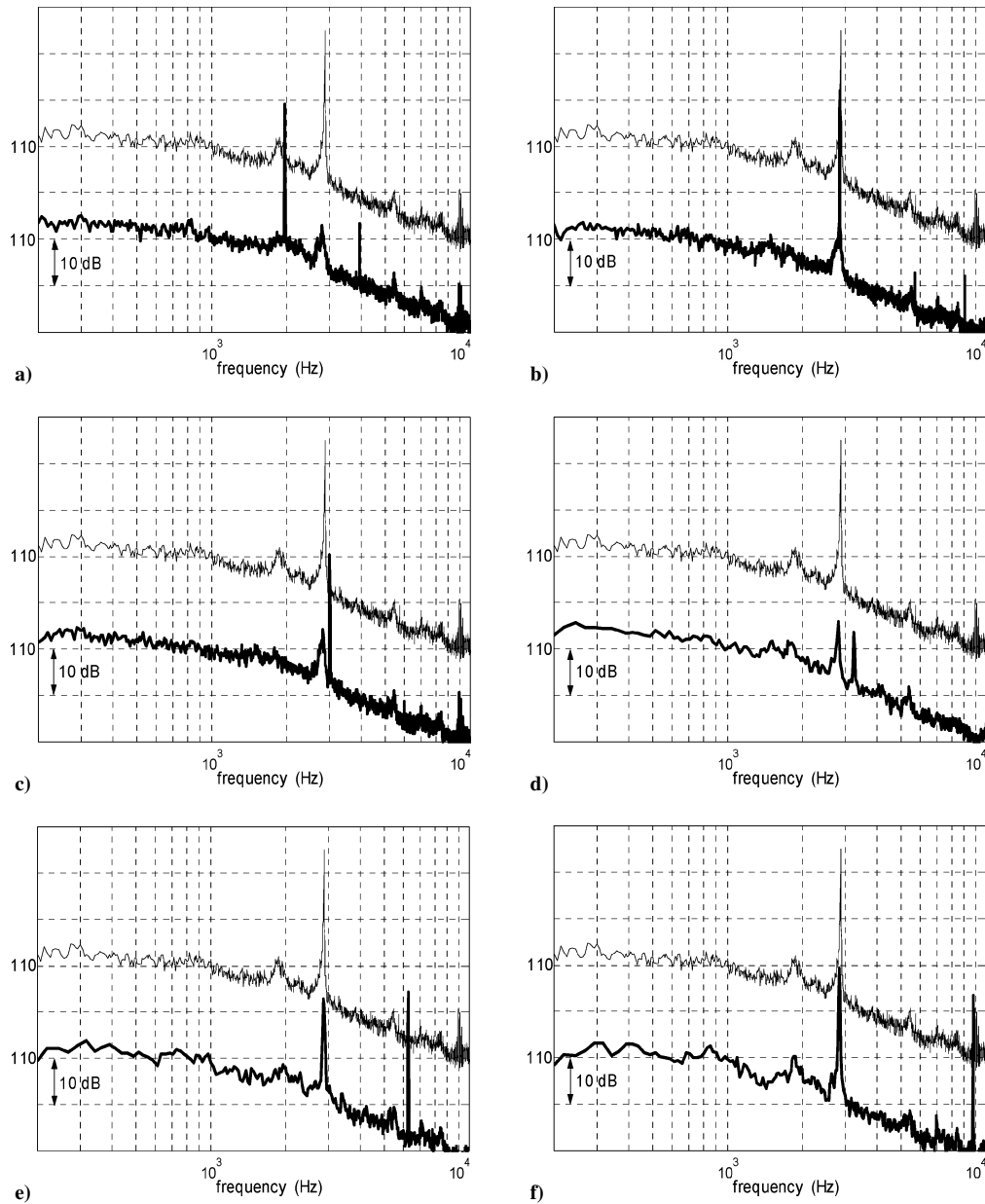


Fig. 7 Effect of forcing frequency on Mach 0.3 flow; upper (thin) line is the baseline flow SPL spectrum, and lower (thick) line is the spectrum with forcing at a) 2.0 kHz, b) 2.8 kHz (resonant frequency), c) 3.0 kHz, d) 3.25 kHz (optimal forcing frequency), e) 6.25 kHz, and f) 9.8 kHz.

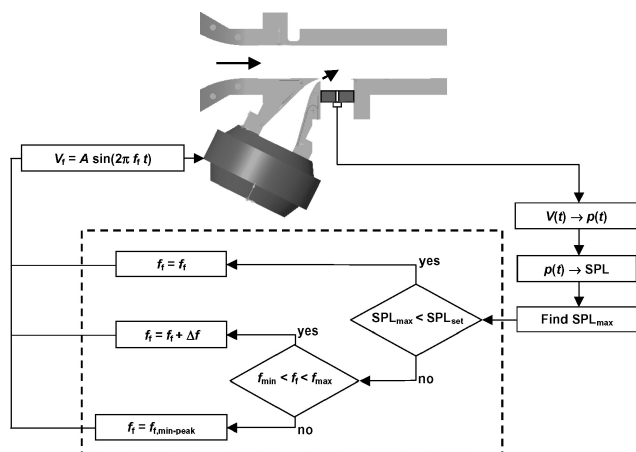


Fig. 8 Schematics of the logic-based type of controller for reduction of cavity flow resonant peaks.

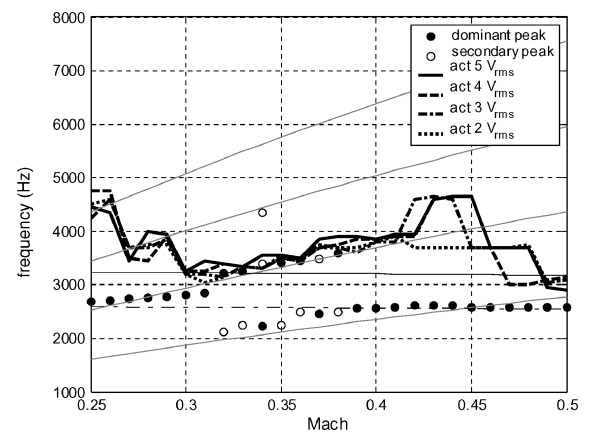


Fig. 9 Resonant frequencies and optimal forcing frequencies to reduce them as a function of the flow Mach number. Visible as thin lines are also the Rossiter frequencies and the frequency of the cavity first longitudinal and transversal modes of Fig. 2.

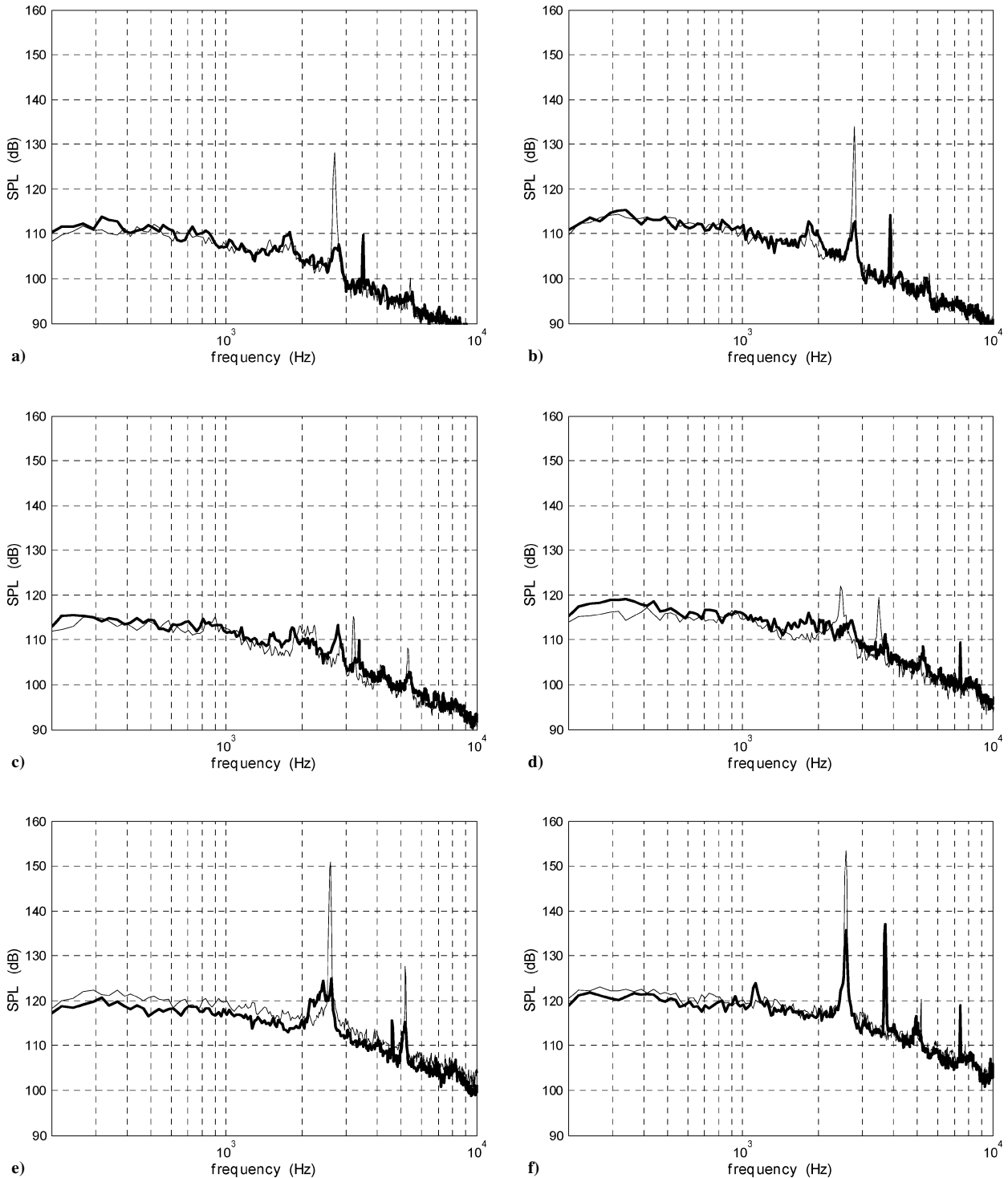


Fig. 10 Noise spectra of the unforced cavity flow (thin line) and of the same flow controlled with optimal frequency forcing at $4 V_{rms}$ (thick line) at selected Mach numbers $M =$ a) 0.26, b) 0.29, c) 0.32, d) 0.37, e) 0.43, and f) 0.46.

Figure 10 shows the effect of optimal frequency forcing on the same flow cases discussed in Fig. 3. For each Mach number case, the thin line shows the same spectrum as in Fig. 3, and the thick line indicates the spectrum with optimal forcing at $4 V_{rms}$. Similar to what was noted in commenting about Fig. 7, forcing has a major effect on reducing the resonant peaks and their harmonics but seems to have little or no effect on the broadband spectral components.

Figure 11 compares the intensities of the highest spectral peak as a function of the Mach number for the unforced flow and for flow with optimal frequency forcing at excitation voltages of 5, 4, 3, and $2 V_{rms}$. The thin continuous and dotted lines show the unforced highest peak

and the low-frequency noise plateau as in Fig. 4. The thick lines refer to the peaks of the optimally forced cases. This figure and Figs. 10a–10d clarify that forcing at optimal frequency eliminates altogether the resonant peaks in the Mach number range 0.25–0.4 irrespective of the actuator excitation voltage, i.e., the velocity at the actuation exit slot. The resulting flow is so devoid of any significant peak that the maximum spectral level basically coincides with the low-frequency noise plateau. At higher Mach numbers especially above 0.45, the original resonant peak is much stronger and only intense actuation at 4 or $5 V_{rms}$ is capable of producing a peak reduction of 10 dB.

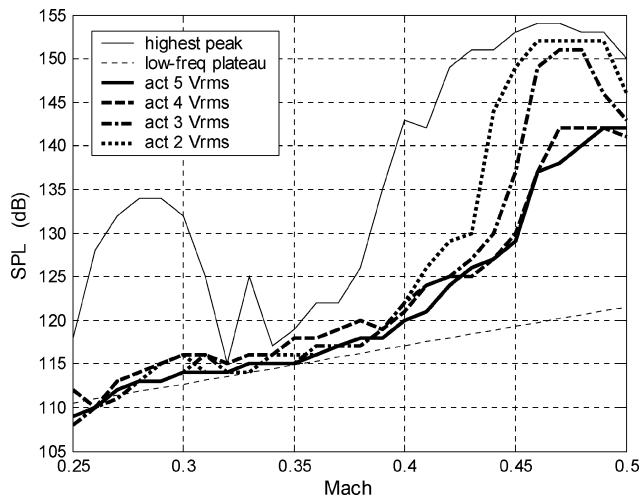


Fig. 11 Intensity of the highest spectral peak of unforced flow and of the flow forced at optimal frequency for peak reduction as a function of the flow Mach number.

VII. Discussion

In this section we further analyze and discuss some of the results from the experiments presented earlier.

First, from Fig. 2 we observe that, in contrast with the observations of Rockwell et al.³ and Williams et al.,⁴ we did not find single-mode resonance to occur around the intersection of the Rossiter modes with the first longitudinal acoustic mode of the cavity, which is around 3.4 kHz. There is also a transversal acoustic mode in the facility (duct mode), which is associated with the depth of the test section from the cavity floor to the top wall of the tunnel.²⁴ The frequency associated with this first transversal acoustic mode is approximately 2.7 kHz. This acoustic mode is also plotted in Fig. 2. The intersections of this mode with the Rossiter modes are close to where we observe single modes. Therefore, it seems that interaction of Rossiter modes with this mode is more dominant in our setup than with the longitudinal mode. This issue will be further studied in the future.

Comparison of the SPL spectra of optimally forced flows (Figs. 7d and 10) with the spectra of multimode resonant flows (Fig. 3c and 3d) suggests that optimal frequency forcing induces in the system a state similar to multimode resonance. In commenting on similar peak reductions obtained with open-loop forcing, Cattafesta et al.¹ suggested that a competition exists between the fundamental mode and the forced mode for the available energy that can be extracted from the mean flow. Analogous conclusions were deduced in successive works by the same authors⁵ and by Williams et al.,⁶ who used joint time-frequency analysis and visual imaging to capture the rapid mode switching in multimode cavity resonance. In these conditions a significant drop of the spectral peaks was observed as the energy switches back and forth among the various Rossiter modes.⁴ We thus hypothesize that forcing at optimal frequency creates a similar switching between the resonant and the forcing modes. Because this switching, although rapid, is not instantaneous, part of the available energy remains in the mean flow. This produces a less efficient resonant system where no single mode locks in to dominate the spectrum. Figure 12, comparing the energy distribution in the time-frequency domain of the resonant and controlled Mach 0.3 flow obtained using the Mexican hat wavelet transformation discussed by Hileman et al.,³⁸ supports this point. In the resonant case (Fig. 12a), high-energy levels centered at the resonant frequency 2.8 kHz repeat continuously in time, a pattern not visible in the case of optimal frequency control (Fig. 12b), for which the energy level is always much lower and seems to switch between frequencies below and above 3 kHz. Calculation of the overall SPL (OASPL) also confirms that optimal frequency forcing produces a less efficient acoustic system. For instance, the OASPL of the Mach 0.3 flow with 4-V_{rms} optimal frequency forcing is 132.0 dB, a lower value than the OASPL of 135.9 dB obtained for the baseline Mach 0.30 flow (Fig. 7d).

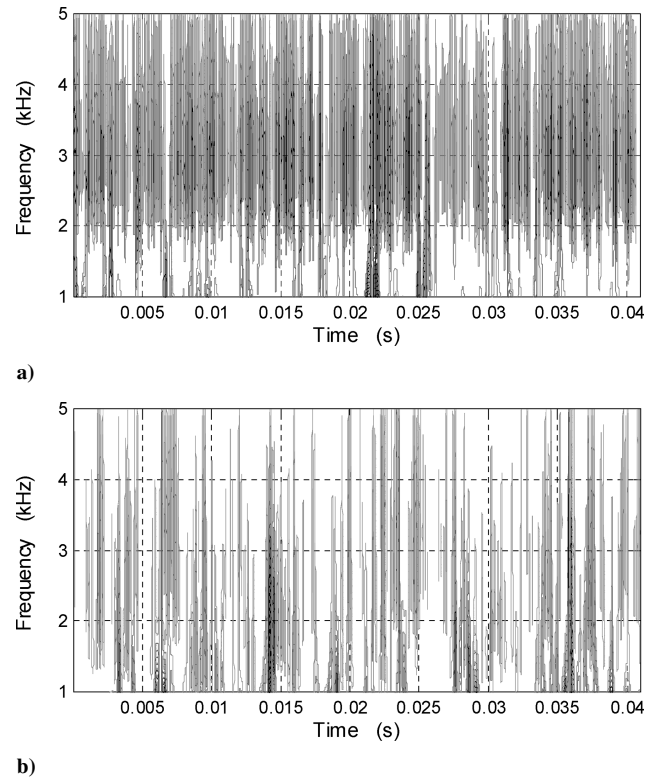


Fig. 12 Energy distribution for the Mexican hat wavelet transformation of time trace excerpts of a) resonant Mach 0.3 cavity flow and b) the same flow controlled with optimal frequency forcing.

Finally, the idea that optimal frequency forcing induces multimode resonance seems also to be supported by the results of Fig. 9 where the optimal forcing frequencies for single-mode resonance tend to coincide with Rossiter modes different from the resonant one while optimal forcing frequencies for multimode resonance coincide with one of the naturally existing modes.

As observed in discussing Fig. 11, optimal frequency forcing becomes less effective as the flow grows stronger above Mach 0.40. It is the authors' belief that this is due to the lack of actuation authority for these more energetic flow conditions. Future use of a more powerful compression driver should alleviate this problem and allow the study of optimal frequency forcing at higher Mach numbers. This seems particularly interesting because, as can be deduced from Fig. 11, above Mach 0.5 the cavity flow should reach another multimode resonance state similar to that observed in the same figure above Mach 0.3.

VIII. Conclusions

A set of experiments for characterizing and controlling the resonance induced by flow over a shallow cavity in the Mach number range of 0.25–0.5 has been presented. Survey of the baseline flow indicates that the flow operates in single-mode resonance in the Mach number ranges of 0.25–0.31 and 0.39–0.5 and multimode resonance in the intermediate Mach number range of 0.32–0.38. Resonant peaks are particularly intense at the higher-Mach-number settings.

A preliminary study of the actuator, limited to the characteristics at its output located just below the leading edge of the cavity, has been performed. The results indicate a frequency-dependent behavior that is not significantly influenced by the presence of the external main flow.

Forcing the flow at different frequencies reveals that the actuator has a strong authority in the frequency range of 2–5 kHz as it is able to disrupt the natural resonant loop and to either tune the flow acoustics to its own frequency or eliminate/substantially reduce all of the peaks/modes. At higher frequencies the actuator progressively loses its authority.

At some frequencies the effect of actuation was to reduce the resonant peak without introducing a peak of its own. Based on these observations, a logic-based type of controller has been devised that searches for the optimal actuation frequency for resonant-peak suppression according to a feedback scheme and then maintains the system in such a state. The controller proved to be effective in reducing strong resonant peaks in all of the Mach number ranges explored.

Extensive data collected in conjunction with the control experiments identify for each Mach number the optimal forcing frequency for reducing the resonant peak. This produces spectra devoid of any significant peak for Mach numbers less than 0.4 irrespective of the actuation input voltage level. At higher Mach numbers significant reductions are obtained only with larger actuation voltages (strong actuation). A mechanism for the physics of peak reduction with optimal frequency forcing is discussed and warrants further future investigation.

Acknowledgments

The support of this work by the Air Force Research Laboratories/Air Vehicle Directorate (AFRL/VA) and Air Force Office of Scientific Research through the Collaborative Center of Control Science (CCCS) (Contract F33615-01-2-3154) is very much appreciated. We thank the rest of the flow control team at CCCS, Hitay Özbay, James Myatt, James DeBonis, Chris Camphouse, Önder Efe, Edgar Caraballo, James Malone, Jesse Little, Xin Yuan, and Peng Yan. We thank David Williams and Lou Cattafesta for fruitful discussions. Finally we gratefully acknowledge the help of James Hileman and Subin Sethuram in implementing the routines for data acquisition and flow control.

References

- ¹Cattafesta, L. N., III, Garg, S., Choudhari, M., and Li, F., "Active Control of Flow-Induced Cavity Resonance," AIAA Paper 97-1804, June 1997.
- ²Rossiter, J. E., "Wind Tunnel Experiments on the Flow over Rectangular Cavities at Subsonic and Transonic Speeds," RAE TR 64037 and Aeronautical Research Council, Repts. and Memoranda No. 3438, 1964.
- ³Rockwell, D., and Naudascher, E., "Review—Self-Sustaining Oscillations of Flow past Cavities," *Journal of Fluids Engineering*, Vol. 100, June 1978, pp. 152–165.
- ⁴Williams, D. R., Fabris, D., and Morrow, J., "Experiments on Controlling Multiple Acoustic Modes in Cavities," AIAA Paper 2000-1903, June 2000.
- ⁵Cattafesta, L. N., III, Garg, S., Kegerise, M. S., and Jones, G. S., "Experiments on Compressible Flow-Induced Cavity Oscillations," AIAA Paper 98-2912, June 1998.
- ⁶Williams, D. R., Fabris, D., Iwanski, K., and Morrow, J., "Closed-Loop Control in Cavities with Unsteady Bleed Forcing," AIAA Paper 2000-0470, Jan. 2000.
- ⁷Cattafesta, L. N., III, Williams, D. R., Rowley, C. W., and Alvi, F. S., "Review of Active Control of Flow-Induced Cavity Resonance," AIAA Paper 2003-3567, June 2003.
- ⁸Heller, H. H., and Bliss, D. B., "The Physical Mechanisms of Flow-Induced Pressure Fluctuations in Cavities and Concepts for their Suppression," AIAA Paper 75-491, March 1975.
- ⁹Sarno, R. L., and Franke, M. E., "Suppression of Flow-Induced Pressure Oscillations in Cavities," *Journal of Aircraft*, Vol. 31, No. 1, 1994, pp. 90–96.
- ¹⁰Ukeiley, L. S., Ponton, M. K., Seiner, J. M., and Jansen, B., "Suppression of Pressure Loads in Cavity Flows," *AIAA Journal*, Vol. 42, No. 1, 2004, pp. 70–79.
- ¹¹Chokani, N., and Kim, I., "Suppression of Pressure Oscillations in an Open Cavity by Passive Pneumatic Control," AIAA Paper 91-1729, June 1991.
- ¹²Stanek, M. J., Raman, G., Kibens, V., Ross, J. A., Odedra, J., and Peto, J. W., "Control of Cavity Resonance Through Very High Frequency Forcing," AIAA Paper 2000-1905, June 2000.
- ¹³McGrath, S. F., and Shaw, L. L., "Active Control of Shallow Cavity Acoustic Resonance," AIAA Paper 96-1949, June 1996.
- ¹⁴Stanek, M. J., Ross, J. A., Odedra, J., and Peto, J. W., "High Frequency Acoustic Suppression—The Mystery of the Rod-in-Crossflow Revealed," AIAA Paper 2003-0007, Jan. 2003.
- ¹⁵DiStefano, J. J., III, Stubberud, A. R., and Williams, I. J., *Feedback and Control Systems*, Schaum's Outlines, 2nd ed., McGraw-Hill, New York, 1990.
- ¹⁶Shaw, L., "Active Control for Cavity Acoustics," AIAA Paper 98-2347, June 1998.
- ¹⁷Grove, J., Leugers, J., and Akroyd, G., "USAF/RAAF F-111 Flight Test with Active Separation Control," AIAA Paper 2003-0009, Jan. 2003.
- ¹⁸Shaw, L., and Northcraft, S., "Closed Loop Active Control for Cavity Resonance," AIAA Paper 99-1902, May 1999.
- ¹⁹Cattafesta, L. N., III, Shukla, D., Garg, S., and Ross, J. A., "Development of an Adaptive Weapons-Bay Suppression System," AIAA Paper 99-1901, May 1999.
- ²⁰Kegerise, M. A., Cattafesta, L. N., III, and Ha, C., "Adaptive Identification and Control of Flow-Induced Cavity Oscillations," AIAA Paper 2002-3158, June 2002.
- ²¹Williams, D. R., Rowley, C. W., Colonius, T., Murray, R. M., MacMartin, D. G., Fabris, D., and Albertson, J., "Model-Based Control of Cavity Oscillations—Part 1: Experiments," AIAA Paper 2002-0971, Jan. 2002.
- ²²Rowley, C. W., Williams, D. R., Colonius, T., Murray, R. M., MacMartin, D. G., and Fabris, D., "Model-Based Control of Cavity Oscillations—Part II: System Identification and Analysis," AIAA Paper 2002-0972, Jan. 2002.
- ²³Rowley, C. W., and Williams, D. R., "Control of Forced and Self-Sustained Oscillations in the Flow past a Cavity," AIAA Paper 2003-0008, Jan. 2003.
- ²⁴Ziada, S., Ng, H., and Blake, C. E., "Flow Excited Resonance of a Confined Shallow Cavity in Low Mach Number Flow and Its Control," *Journal of Fluids and Structures*, Vol. 18, No. 1, 2003, pp. 79–92.
- ²⁵Cabell, R. H., Kegerise, M. A., Cox, D. E., and Gibbs, G. P., "Experimental Feedback Control of Flow Induced Cavity Tones," AIAA Paper 2002-2497, June 2002.
- ²⁶Gad-el-Hak, M., *Flow Control—Passive, Active, and Reactive Flow Management*, Cambridge Univ. Press, New York, 2000.
- ²⁷Schaeffler, N. W., Hepner, T. E., Jones, G. S., and Kegerise, M. A., "Overview of Active Flow Control Actuator Development at NASA Langley Research Center," AIAA Paper 2002-3159, June 2002.
- ²⁸Cain, A. B., Rubio, A. D., Bortz, D. M., Banks, H. T., and Smith, R. C., "Optimizing Control of Open Bay Acoustics," AIAA Paper 2000-1928, June 2000.
- ²⁹Stanek, M. J., Raman, G., Ross, J. A., Odedra, J., Peto, J., Alvi, F., and Kibens, V., "High Frequency Acoustic Suppression—The Role of Mass Flow, the Notion of Superposition, and the Role of Inviscid Instability—A New Model (Part II)," AIAA Paper 2002-2404, June 2002.
- ³⁰Raman, G., and Kibens, V., "Active Flow Control Using Integrated Powered Resonance Tube Actuators," AIAA Paper 2001-3024, June 2001.
- ³¹Raman, G., Mills, A., Othman, S., and Kibens, V., "Development of Powered Resonance Tube Actuators for Active Flow Control," Proceedings of the American Society of Mechanical Engineers—Fluids Engineering Div. Summer Meeting, 2001-18273, May–June 2001.
- ³²Kastner, J., and Samimy, M., "Development and Characterization of Hartmann Tube Fluidic Actuators for High-Speed Flow Control," *AIAA Journal*, Vol. 40, No. 10, 2002, pp. 1926–1934.
- ³³McCormick, D. C., "Boundary Layer Separation Control with Directed Synthetic Jets," AIAA Paper 2000-0519, Jan. 2000.
- ³⁴Samimy, M., Debiassi, M., Caraballo, E., Özbay, H., Efe, M. Ö., Yuan, X., DeBonis, J., and Myatt, J. H., "Closed-Loop Active Flow Control—A Collaborative Approach," AIAA Paper 2003-0058, Jan. 2003.
- ³⁵Seifert, A., and Pack, L. G., "Oscillatory Control of Separation at High Reynolds Numbers," *AIAA Journal*, Vol. 37, No. 9, 1999, pp. 1062–1071.
- ³⁶Chen, F.-J., Yao, C., Beeler, G. B., Bryant, R. G., and Fox, R. L., "Development of Synthetic Jet Actuators for Active Flow Control at NASA Langley," AIAA Paper 2000-2405, June 2000.
- ³⁷Guy, Y., McLaughlin, T. E., and Albertson, J. A., "Effect of Geometric Parameter on the Velocity Output of a Synthetic Jet Actuator," AIAA Paper 2002-0126, Jan. 2002.
- ³⁸Hileman, J., Thurow, B., and Samimy, M., "Exploring Noise Sources Using Simultaneous Acoustic Measurements and Real-Time Flow Visualization in Jets," *AIAA Journal*, Vol. 40, No. 12, 2002, pp. 2382–2392.

R. Lucht
Associate Editor